Appl Phys B (2011) 104:569–576
DOI 10.1007/s00340-011-4599-8

Applied Physics B
Lasers and Optics

A high-energy, chirped laser system for optical Stark deceleration

N. Coppendale · L. Wang · P. Douglas · P.F. Barker

Received: 13 October 2010 / Revised version: 21 April 2011 / Published online: 10 June 2011

Abstract We describe a high-energy, frequency chirped laser system designed for optical Stark deceleration of cold molecules. This system produces two, pulse amplified beams of up to 700 mJ with flat-top temporal profiles, whose frequency and intensity can be well controlled for durations from 20 ns–10 μs. The two beams are created by amplifying a single, rapidly tunable Nd:YVO_4 microchip type laser at 1064 nm, which can be frequency chirped by up to 1 GHz over the duration of the pulse. Intensity modulation induced by relaxation oscillations in the microchip laser during the frequency chirp are virtually eliminated by injection locking a free running semiconductor diode laser before pulsed amplification.

1 Introduction

The creation and manipulation of the center-of-mass motion of cold molecules [1–4] allows the study of molecular interactions that are masked at higher temperatures. This includes many body dipole–dipole physics, exotic quantum phases [5] and chemistry that is dominated by resonance and tunneling phenomena [6]. The low translational energy of cold molecules allows trapping by electrostatic or magnetic fields for long periods, enabling spectroscopy at the highest resolution [7]. Such precision measurements have application in molecular physics but also in tests of physics beyond the standard model [8] and the search for parity violation at the molecular level [9]. Some simple diatomic molecular species can be created by association of laser cooled species [10, 11]. However, a wider range of much more complex species can be created by filtering out a narrow velocity distribution from a molecular beam using conservative fields [12]. Magnetic, electrostatic and optical fields have been used in this way to decelerate and trap molecules [13–15]. Zeeman and Stark deceleration utilize molecules with permanent magnetic and electric dipole moments, respectively, to slow molecules.

Optical Stark deceleration uses intense optical fields to induce a dipole moment which interacts with the field that created it to produce an optical potential. The gradient in the optical potential has sufficient force to slow molecules and atoms. To date this method has been used to slow nitric oxide (NO) and benzene (C_6H_6) molecules [16–18] to rest in a backing gas of xenon. The force that can be applied to molecules is proportional to the intensity gradient such as in a tightly focused laser beam [19]. A larger gradient can be created by the interference pattern formed by two near counter-propagating laser beams. The optical potential formed by the interaction of the interference pattern with the polarizability of the molecules, produces a periodic potential called an optical lattice. A fixed frequency difference between the two beams creates a constant velocity lattice which has been used to decelerate molecules using a half oscillation of the molecule trapped in the deep optical lattice. Intensities in 10^{12}–10^{14} W/cm^2 range are used to create the lattice which can have a well depth of $E/k_b = 1000$ K, where k_b is Boltzmann's constant. When the lattice velocity is half that of the molecular beam, molecules can be decelerated from 400 m/s to zero velocity in the laboratory frame on time scales of a few nanoseconds. This scheme is, however, limited to the creation of slowed molecular ensembles with an energy spread that is comparable to the initial spread of the molecular beam. In addition, a fast switching of the optical field is technically challenging. While a narrower energy

N. Coppendale · L. Wang · P. Douglas · P.F. Barker (✉)
University College London, Gower Street, London WC1E 6BT, UK
e-mail: p.barker@ucl.ac.uk

spread, centered at 0 m/s, can be created by trapping these molecules with a lower trap depth than the decelerating potential, it is not suitable for high resolution collision studies at arbitrary velocities which require a narrow energy spread.

A narrower energy spread can be accomplished by the application of shallower optical potentials, which instead of moving at constant velocity is constantly decelerated. In this scheme an optical lattice traps and transports the molecules to zero velocity. This has been described theoretically [20, 21] where a linear frequency chirp is used to create a lattice with a constant deceleration, over time scales on the order of hundreds of nanoseconds. This optical potential is given by

$$U(y,t) = -\frac{\alpha}{\epsilon_0 c}\sqrt{I_1(y,t)I_2(y,t)}\cos^2\left(qy + \omega_0 t - \frac{1}{2}\beta t^2\right), \tag{1}$$

where α is the polarizability of the species, $q = \frac{4\pi}{\lambda}\sin(\theta/2)$ is the lattice wave vector, ω_0 is the initial frequency difference between the two beams, and $\beta = (d\omega/dt)$ is the chirp rate. The time dependent frequency difference between the two beams determines the velocity of the optical lattice. To create a lattice which starts at the speed of the molecular jet and decelerates down to zero velocity, requires a frequency excursion of approximately 1 GHz for nearly counter-propagating beams, over 20–1000 ns [20, 21]. A flat-top temporal intensity profile is required for the deceleration period to maintain the lattice well depth. This ensures that no molecules are lost during the deceleration period.

In this paper we describe a laser system that we have developed for chirped optical Stark deceleration of molecules. It uses pulsed amplification of a continuous wave (CW) chirped Nd:YVO_4 laser, which produces a low intensity beam which can have an arbitrary frequency chirp. This low power CW laser is split into two time delayed beams which are subsequently pulse amplified in a commercial (Continuum Lasers) flash lamp pumped Nd:YAG amplifier system to produce a flat-top temporal profile. The amplified pulses have essentially the same frequency characteristics of the two time delayed CW beams. This system is capable of intensities in the (10^{10}–10^{11} W/cm^2) range required for the deceleration of molecules. We demonstrate amplified pulses of 140 ns duration, with chirp excursions in excess of 10 GHz/μs that are suitable for deceleration of cold molecules in a molecular beam.

2 Overview of laser system

The laser system developed for chirped optical Stark deceleration is shown in Fig. 1. The two CW beams that are input into the amplifiers are split from the same single mode

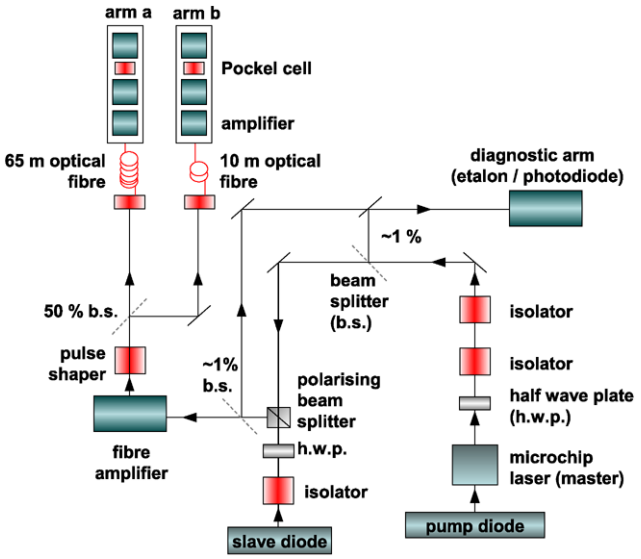

Fig. 1 A schematic of the high-energy chirped laser system. A microchip laser (master) injection locks a free running 'slave' diode whose output is coupled into a fiber amplifier. A pulse shaper creates pulses of width in the 20–1000 ns range. The pulsed beam is split into two arms and coupled into two optical fibers of different lengths. These delayed beams are fed into each arm (*A* and *B*) of a flash lamp pumped Nd:YAG amplifier

output of a Nd:YVO_4 microchip laser (master) which can be rapidly frequency chirped by an intra-cavity electro-optic crystal. The output of this laser system produces an output power of ≈10 mW at a wavelength of 1064 nm. This light is used to injection lock a free running semiconductor diode laser, which is called the slave laser. This produces a frequency and intensity controlled output that is coupled into a commercial fiber amplifier (IPG model no. YAR-1K-LP-SF). This amplifies our CW beam to 1 W. A commercial electro-optic pulse shaper (Kentech Instruments) in combination with a polarizer, is used as a variable attenuator to chop up this beam into pulses of 20–1000 ns duration, which are then split and coupled into two optical fibers of different lengths. Each pulse from the fiber is amplified by a flash lamp pumped, pulsed amplifier denoted by arms *A* and *B* as shown in Fig. 1. A Pockels cell and a polarizer combination is used as a fast shutter in each arm, before the final stage of amplification, to prevent amplified spontaneous emission. A difference in fiber length of 55 m creates a time delay in the output of the laser system of 275 ns. Using this delay, a single laser can be used to create a chirped frequency difference.

2.1 Master microchip laser

A common way to rapidly tune the frequency of a laser system is to change the optical cavity length using an electro-optic crystal placed inside the cavity or by modulating the current in a semiconductor laser. For frequency excursions

of ≈1 GHz, a small cavity (<1 cm) with a large free spectral range >1 GHz is required. Such schemes have been implemented using external cavity diode lasers [22] and small solid state lasers using microchip technology [23]. To provide a chirped master laser for amplification to the energies required for optical Stark deceleration, we have built a short cavity (4.5 mm), single frequency Nd:YVO_4 laser, operating at a wavelength of approximately 1064 nm as shown in Fig. 2. The cavity consists of a 500 μm thick Nd:YVO_4 microchip (CASIX) with a high reflecting reflective coating for 1064 nm and an anti-reflection coating for the pump wavelength of 808 nm on one side of the microchip crystal and an anti-reflection coating for 1064 nm and 808 nm on the other. The microchip is thermally attached to a copper block, the temperature of which is controlled to within 10 mK by a Peltier cooler. A 94% reflective plane mirror forms the output coupler of the cavity while an intra-cavity electro-optic crystal ($LiTaO_3$) crystal ($n_2 = 2.2$) of length 3 mm is placed in the center of the cavity. When a voltage is applied to the electro-optic crystal, the change in optical path length allows a rapid change in the laser frequency. The output power of this laser system is approximately 10 mW. The frequency change δf of the laser with applied voltage δV to the electrodes of the $LiTaO_3$ crystal is given by [24]

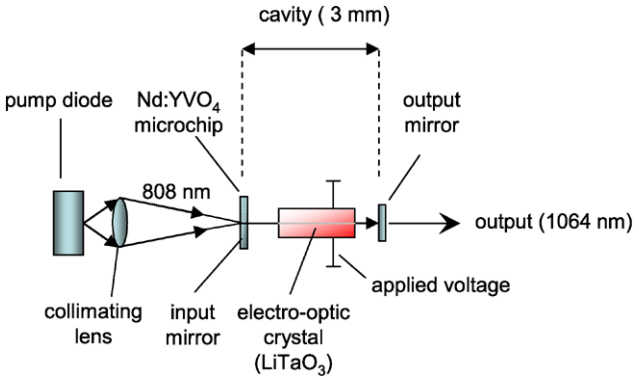

Fig. 2 A schematic of microchip laser. The cavity is formed by a 500 μm thick Nd:YVO_4 microchip with a high reflecting reflective coating for 1064 nm and anti-reflection coating for the pump wavelength of 808 nm. A 94% reflective output mirror forms the output coupler of the cavity. An intra-cavity electro-optic crystal ($LiTaO_3$) crystal $n_2 = 2.2$ of length 3 mm is used to rapidly change the optical path length

$$\delta f = \frac{\eta n_1^2 r_{33} f_{\text{opt}}}{2d} \frac{n_1 l_1}{n_1 l_1 + n_2 l_2 + n_3 l_3} \delta V, \tag{2}$$

where l_1, l_2 and l_3 are the respective lengths of the $LiTaO_3$ crystal, the Nd:YVO_4 crystal and the air gap. The overlap efficiency between the electric field and laser cavity mode is given by η and d is the thickness of the $LiTaO_3$ crystal. The refractive index of the extraordinary wave in the $LiTaO_3$ crystal is n_1 and the refractive index of the π polarization component Nd:YVO_4 is n_2. The refractive index of air is n_3. The electro-optic coefficient of the $LiTaO_3$ crystal along the cavity axis is r_{33} (30.4 pm/V) at 1064 nm and f_{opt} is the frequency of the optical wave.

We require a continuous tuning range of approximately 1 GHz for molecular deceleration and operation on a single longitudinal and transverse mode. The shortest possible cavity length maximizes the mode hop free tuning range, while having a larger electro-optic crystal which forms the majority of the cavity length ($n_1 l_1 \gg n_2 l_2 + n_3 l_3$) increases the frequency change per voltage which is applied to the crystal (tunability, $f_V = \Delta f / \Delta V$). However, increasing the length of the crystal would increase the tunability but also reduce the mode hop free tuning range for a particular pump intensity. We determine the tunability of the laser by measuring the change in laser frequency as a function of applied voltage. Figure 3 shows the frequency shift as a function of

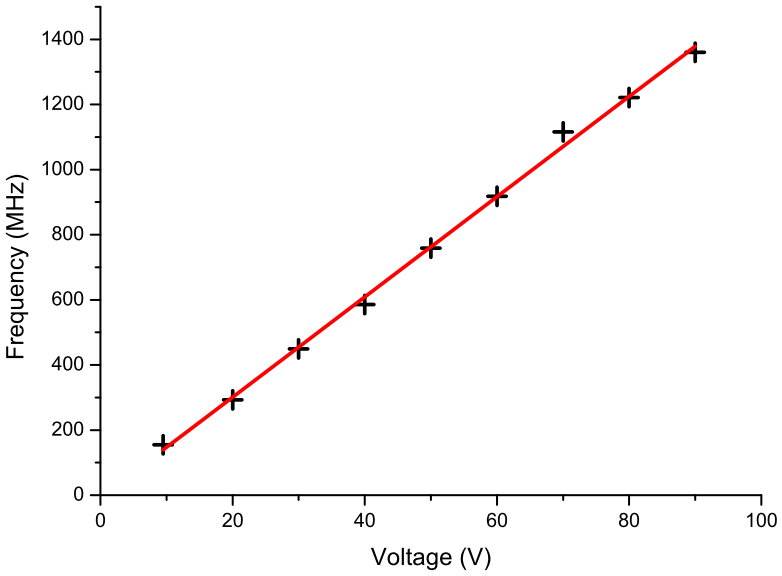

Fig. 3 Frequency change of the Nd:YVO_4 microchip laser as a function of voltage applied to intra-cavity electro-optic crystal. A linear fit gives a tunability of 15.4 ± 0.3 MHz/V

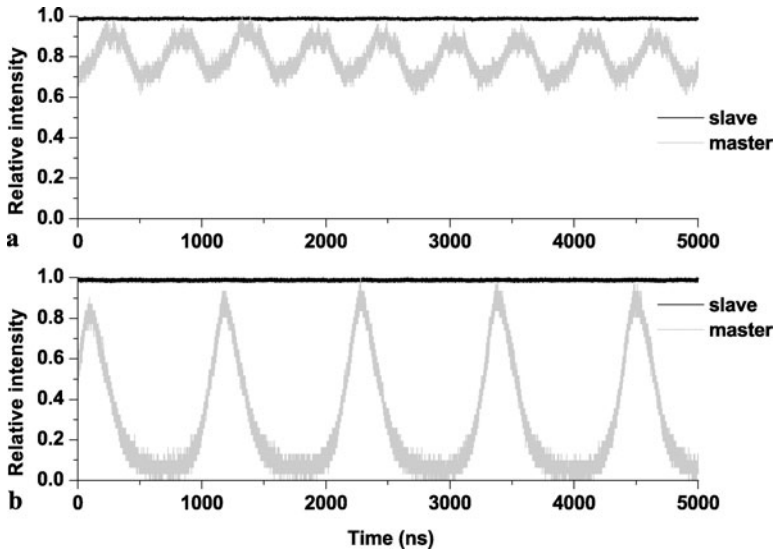

Fig. 4 (**a**) A plot of the master and slave intensity as a function of time, when a sinusoidal voltage with amplitude ≈70 V is applied to the electro-optic crystal at a frequency of 1825 kHz. Intensity modulation of <30% can clearly be seen of the master laser at a frequency similar to the chirp. After injection into the slave this modulation is reduced to effectively zero (<2%). Intensity noise limits further resolution in the measurement of this modulation. (**b**) A plot of master and slave intensity as a function of time when the voltage applied is modulated at 902 kHz. At this frequency there is a resonance with the relaxation oscillations inherent in the laser system and thus the modulation is much greater, down to almost zero intensity and up to three times the unmodulated intensity. After injection into the slave diode, the intensity modulation is reduced to effectively <2%

applied d.c. voltage as measured by the fringe shift in a confocal etalon with free spectral range =1.4 GHz, and a finesse of 200. There is a linear relationship between the voltage applied and frequency shift with $f_V = 15.4 \pm 0.3$ MHz/volt. We find that our cavity remains single mode up to a D.C. frequency shift of 16.8 GHz, which corresponds to 1090 V for $f_V = 15.4$ MHz/V.

3 Reducing the effects of relaxation oscillations

Rapid changes in the frequency of the laser also induce relaxation oscillations. These are observed as large periodic modulations in the intensity of the laser output which occur due to the large difference between the cavity lifetime, ($\tau_c = 300$ ps) and the excited state lifetime ($\tau_2 = 90$ µs). The characteristic relaxation oscillation frequency of the laser is given by

$$\omega_{\mathrm{sp}} = \sqrt{\frac{r-1}{\tau_c} \times \frac{1}{\tau_2}} \tag{3}$$

where r is the ratio of the pumping rate to the threshold pumping rate. This equation predicts a relaxation oscillation frequency of 685 kHz for $r = 1.5$ for our laser.

When the modulation frequency of the voltage applied to the electro-optic crystal is comparable to the relaxation oscillation frequency, stronger intensity oscillations are induced. Additionally, there are many acoustic resonances in the electro-optic crystal, which are also induced by the voltage modulation. They typically occur above 80 kHz and have been observed up to 25 MHz. [25]. At some modulation frequencies the intensity modulations due to relaxation oscillations can be nearly 100% of the output intensity.

Such intensity oscillations are not suitable for optical Stark deceleration and must be removed. A typical way to suppress these oscillations is to use electronic feedback to the current of the pump diode [26] so that when the intensity is low the current is driven higher. While this was successful in suppressing an intensity modulation of 10%, it was insufficient to prevent the larger intensity oscillations induced by the chirp. To remove these oscillations we use an injection locking scheme where our CW chirped laser provides the master frequency source whose output is coupled into a slave laser. The frequency of the slave is now determined by the chirped laser but its intensity is in principle constant in time. Additionally, the slave laser is a free running semiconductor diode laser which has typical relaxation oscillation frequencies in the GHz regime [27]. As these are much larger than those at the MHz relaxation oscillation frequencies of the master laser, it is unlikely these oscillations will be induced in the slave.

Figure 4 shows the output intensity of the master and slave laser when the voltage that is applied to the electro-optic crystal is modulated at two frequencies. Figure 4a is the intensity output for an applied voltage of amplitude ≈70 V at a frequency of approximately 1825 kHz and Fig. 4b is for 900 kHz. The grey traces in Figs. 4a

and 4b show the resulting intensity modulation of the master laser due to relaxation oscillations induced by the voltage modulation. The black traces represents the significantly reduced output intensity modulation of the slave laser. At both frequencies the slave intensity modulation is less than 2%. We choose to modulate the frequency of the master laser at 1825 kHz where the intensity oscillations are lowest (Fig. 4a). The slave locks to the instantaneous master laser frequency provided the free running slave is operating within a few GHz [28] of the master's frequency. As in similar systems, the intensity of the oscillations of our slave laser is several orders of magnitude less than the oscillations of the master [22]. The slave remained locked to the master when chirped to a frequency excursion of ≈1390 MHz corresponding to 90 V applied to the electro-optic crystal.

4 CW frequency chirp

To measure the induced chirp of the master-slave and fiber amplifier system, the output of the slave is split into two beams and coupled into two fibers of different lengths. This creates a time delay, and therefore a frequency difference, between the two beams at the fiber outputs when the laser is chirped. This is illustrated in Fig. 5 which shows the frequency shift induced by the applied voltage at the output of each fiber. This chirp is produced by applying a sinusoidal voltage of amplitude 67.5 V to the electro-optic crystal at a frequency of 1825 kHz. Due to the time delay (275 ns) introduced by the difference in fiber lengths, there is a π phase shift between these waveforms. The third trace represents the frequency difference between these two beams that would be observed by heterodyning the two outputs. The maximum frequency difference between the two outputs is 1080 MHz based on a tunability, f_V of 16 MHz/V. At approximately 140 ns and 420 ns the relative frequency between the two arms goes to zero.

To heterodyne the outputs from each fiber, we combine both beams onto a beamsplitter and focus these overlapped beams onto a fast photo-diode with a bandwidth of 2 GHz. The photo-diode signal is recorded on an oscilloscope with a 3 GHz bandwidth. This signal is shown in Fig. 6a and the voltage applied to the electro-optic crystal is shown by the overlaid black line in Fig. 6a. The maximum beat frequency occurs at minimum (or maximum) applied voltage corresponding to 0 ns and 280 ns where the amplitude modulation is at a minimum. The variation in modulation contrast of the beat signal as a function of frequency is due to the non-linearity of the frequency response of the photo-diode. This was determined by measuring the modulation depth as a function of a fixed frequency difference. We assume the electric field of arms A and B are given by $E_{A,B}(t) = E_{A0,B0(t)} \exp[i(\phi_{A,B(t)} + \omega t)]$ where $E_{A,B}$

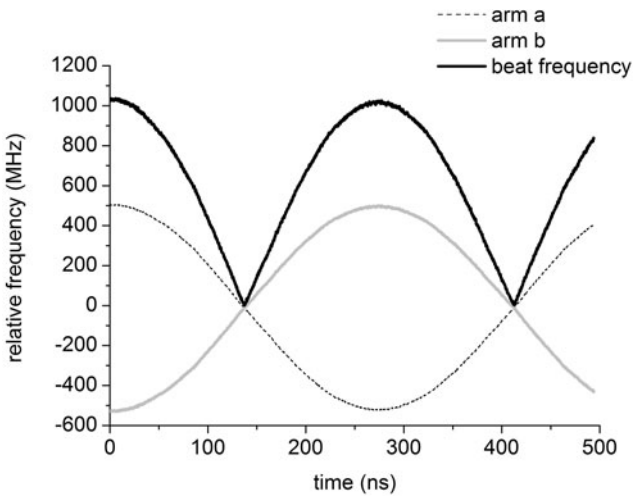

Fig. 5 A plot of the predicted frequency chirp of 1040 MHz, produced by applying a sinusoidally varying voltage with amplitude 67.5 V and creating a π phase delay between the sinusoidally varying frequency of each arm that results from the difference in length between the two arms

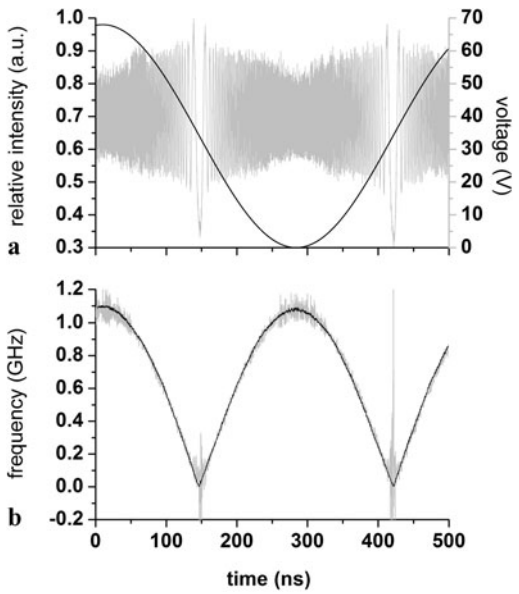

Fig. 6 (**a**) The recorded heterodyne signal and the voltage applied to the electro-optic crystal as a function of time. The voltage was modulated at 1825 kHz, with a peak to peak amplitude of 67.5 V. The frequency dependent variation of the modulation contrast is due to the non-linearity of the frequency response of the photo-diode. (**b**) The instantaneous frequency as a function of time determined from the data shown in (**a**) can be determined to within ±10 MHz, indicating a chirp of 1080 MHz, and a tunability of 16 MHz/V

are the electric field amplitude of each arm oscillating at the same optical frequency ω with a time dependent phase $\phi_{A,B}(t)$ whose derivative with time gives the instantaneous frequency change. To determine the frequency difference between the two beams as a function of time, we used the method of Fee et al. [29] where the beat signal from the

two beams recorded by the photo-diode can be written in the time domain form as

$$V \propto \left|E_A(t)\right|^2 + \left|E_B(t)\right|^2 + E_A(t)E_B^*(t)\exp\left[i\left(\phi_A(t) - \phi_B(t)\right)\right] + c.c. \quad (4)$$

When the beat frequency between the two beams is higher than the Fourier components of the two first terms in the equation above we can determine the instantaneous frequency difference between the beams by first Fourier transforming the beat signal and then applying a bandpass filter to extract only the higher frequency Fourier components of the third term in the equation above. This filtered signal in the frequency domain is transformed back into the time domain and the instantaneous frequency is determined from its time derivative.

Figure 6b represents the instantaneous frequency as a function of time determined from the data shown in Fig. 6a. We cannot accurately determine the instantaneous frequency difference at frequencies below 100 MHz because the envelope of the two lattice fields, represented by the first two terms in (4), also has frequency components in this range. At frequencies above 100 MHz, however, the instantaneous frequency can be determined within ± 10 MHz. Although not performed here, the chirp at lower frequencies could be measured by offsetting the frequency of one of the beams using an acousto-optic modulator. The figure does show that a frequency excursion in excess of 1000 MHz can be attained with our laser. This is more than sufficient for our purposes since it is equivalent to a maximum lattice velocity of >530 ms^{-1} produced by the two counter-propagating beams. This velocity is greater than the initial velocity of cold molecules produced by a cold molecular beam produced by a xenon carrier gas. To derive the tunability, we then fit the function $f = f_V V|\cos\omega t|$ to the derived instantaneous frequency and determine a value of $f_V = 16 \pm 0.5$ MHz/V at a modulation frequency of 1825 kHz. Within the uncertainty of our measurements this value is in good agreement with the d.c. tunability determined from the measurements shown in Fig. 3.

5 Pulse amplification

5.1 Shaping and temporally overlapping of high intensity pulses

To produce the high intensities needed (10^{12}–10^{14} W/cm^2) to create a decelerating lattice, we pulse amplify in a single pass, the output of each fiber using a custom built Nd:YAG system (Continuum lasers). Each arm consists of three flash lamp pumped Nd:YAG rods (100 mm long and 6 mm diameter). The output from the fibers is continually chirped as shown in Fig. 6 but we amplify for the time period that corresponds to the time taken to chirp from the maximum frequency difference between the two beams down to zero. This corresponds to $t_d = 138$ ns, as shown in Fig. 5. To accomplish this we synchronize the voltage modulation of the crystal, and therefore the chirp, with the firing of the flash lamps. As we only require amplification for the duration of the chirp, we use a Pockels cell and polarizer as a pulse shaper, to pass only light for this period of time. We typically produce pulses in the 100–200 ns range with a flat-top temporal profile after amplification. A input pulse with a shape that is well approximated by an exponential rise is required to compensate for the time varying gain saturation effects in the Nd:YAG amplifying rods during amplification.

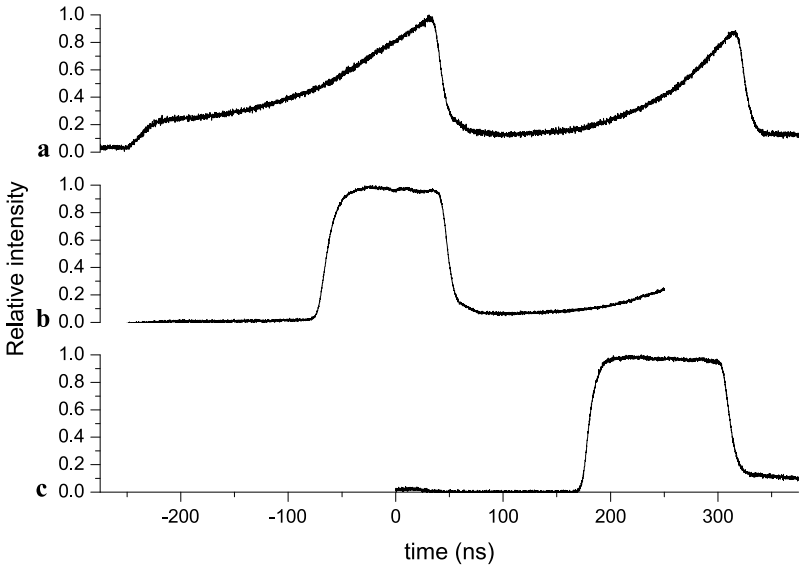

Fig. 7 (**a**) Intensity profile of the light produced by the pulse shaper before input into the fibers and pulse amplified. (**b**) Amplified output from arm A, offset in time for comparison with input pulse (**a**). (**c**) Amplified output from arm B, offset in time for comparison with input pulse (**a**)

As there is a time delay introduced by propagation through the two fibers of different lengths which feed amplifier arms A and B, we are able to use a single pulse shaper to produce two temporally delayed pulses before the CW beam is split, and coupled into the two fibers. The time delay in the fibers brings the first pulse exiting the longer fiber into temporal coincidence with the second pulse from the shorter fiber. The first pulse in the shorter fiber is blocked by a Pockels cell and polarizer before the final amplification stage shown in Fig. 1. The second pulse from the longer fiber is also amplified but at a lower intensity since the gain is largely depleted by the first pulse. Since the temporally overlapped pulses are formed from two temporally delayed pulses originating from the slave, a frequency difference in the outputs results when the master laser is chirped.

Figure 7a shows the intensity profile for two pulses, of different duration, that are sent into each fiber and subsequently pulse amplified. Figures 7b and 7c are the relative intensity recorded for each arm after amplification showing that a near flat-top temporal profile can be achieved. For comparison each profile has been offset in time to compare each output pulse with its respective input shown in Fig. 7a. Although not shown here these two pulses are temporally overlapped when they exit the amplifiers so that they can be used to form a lattice. In comparing the input and output pulses of arm A, it can be seen that input pulse is more than twice as long as the output pulse. This occurs because a Pockels cell is used to hold off amplification until -75 ns when the light is of sufficient intensity. This function can also be fulfilled by the pulse shaper, however, fine tuning ($\approx$ns resolution) of the intensity profile, shown in Fig. 7b, is more easily accomplished by varying the Pockels cell triggering time. The same process is also used to control the amplified intensity profile of arm B, shown in Fig. 7c.

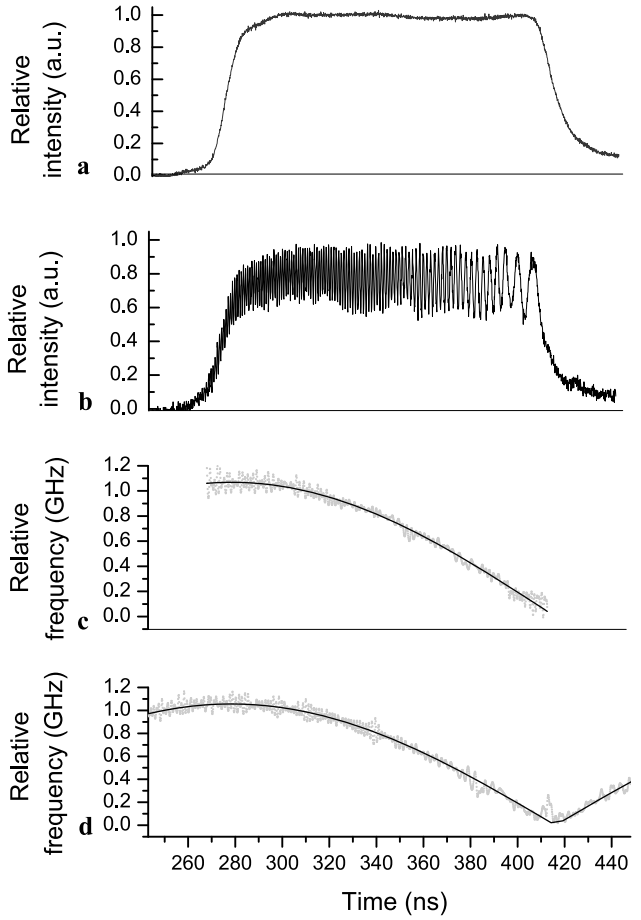

Fig. 8 (**a**) Input profile of one of two the laser beams which are heterodyned on a photo-diode. (**b**) The beat pattern detected on a photo-diode due to sinusoidal chirp with frequency 1.82 MHz and amplitude 74.0 ± 0.05 V. (**c**) Instantaneous frequency as a function of time determined from the data in (**b**) within an uncertainty of ± 10 MHz. Applying a fit to these data indicates a tunability, $f_V = 14.4 \pm 0.2$ MHz/V. (**d**) Instantaneous frequency as a function of time for identical un-amplified continuous wave case for comparison. The same fit indicates $T_c = 14.3 \pm 0.2$ MHz/V which is consistent with the measured tunability in the pulsed case

5.2 Characterization of chirped pulsed amplification

Figure 8a is a temporal profile of one of the two input beams. The outputs of arms A and B of equal pulse duration ($t_d = 140$ ns) are heterodyned to produce a beat pattern as shown in Fig. 8b. The envelope of the beat pattern does not have a flat-top profile because, as explained earlier, the frequency response of the photo-diode is not constant over all frequencies sampled. Figure 8c is the instantaneous frequency difference between the two arms derived from Fig. 8b. The frequency chirps from over 1 GHz down to 0 at a rate of $\approx$8 GHz/μs. The uncertainty in the downward chirp in the central region of the plot where the signal to noise is lowest is <10 MHz. Overlaid with this waveform is a fit to the instantaneous frequency determined by the sinusoidal voltage applied to the electro-optic crystal with amplitude of 74 ± 0.25 V. This has the form $F(t) = V_0 f_V |\cos(\omega t + \phi)|$, where V_0 is the voltage amplitude, f_V is the tunability (MHz/V), and ϕ is simply an arbitrary phase. This indicates a tunability $f_V = 14.4 \pm 0.2$ MHz/V in good agreement with that determined from the rapid CW chirp measurements shown in Fig. 8d where a similar fit indicates a tunability of $f_V = 14.3 \pm 0.2$ MHz/V for the same voltage applied to the e.o. crystal. Importantly, the good agreement in both the fit and the tunability of the CW and pulse amplified beams indicates that no significant additional chirp is introduced by the amplification of the CW seed beams and that this system is suitable for chirped optical Stark deceleration.

6 Conclusions

We have described the development of a high-energy, chirped laser system for the deceleration of molecules within a molecular beam. Central to this system is a CW rapidly tunable Nd:YVO_4 microchip laser operating at 1064 nm, which can be chirped in excess of 7.1 GHz/μs using an intra-cavity electro-optic crystal. Relaxation oscillations induced in this laser system by the rapid chirp are largely removed by injection seeding a free running semiconductor diode laser. The two beams for chirped deceleration are created by introducing a time delay by splitting the chirped CW beam and propagating it into two different length fibers. This allowed us to create two beams with a well defined, time dependent, frequency difference between them. To produce the high-energy, chirped beams with the same frequency characteristics as the CW seed beams we pulse amplified each beam in two separate arms of a single pass flash lamp pumped Nd:YAG amplifier. Each amplified beam had a flat-top temporal profile over 140 ns with an energy per pulse of up to 400 mJ. Although longer flat-top pulses can be created up to 10 μs the length is limited by the difference in fiber length and the coherence of the laser. While our laser system has been developed for optical Stark deceleration of molecules, the ability to produce a rapid and arbitrary chirped output at high-energy output with a controlled pulse shape could be used for high speed spectroscopic measurements in laser based diagnostics of combustion and flow.

References

1. T. Köhler, K. Góral, P. Julienne, Rev. Mod. Phys. **78**, 1311 (2006)
2. K. Jones, E. Tiesinga, P. Lett, P. Julienne, Rev. Mod. Phys. **78**, 483 (2006)
3. J.D. Weinstein, R. deCarvalho, T. Guillet, B. Friedrich, J.M. Doyle, Nature **395**, 148 (1998)
4. H.L. Bethlem, A.J.A. van Roij, R.T. Jongma, G. Meijer, Phys. Rev. Lett. **88**, 133033 (1998)
5. K. Winkler, G. Thalhammer, F. Lang, R. Grimm, J. Hecker Denschlag, A.J. Daley, A. Kantian, H.P. Büchler, P. Zoller, Nature **441**, 853 (2006)
6. N. Balakrishnan, A. Dalgarno, Chem. Phys. Lett. **341**, 652 (2001)
7. T.N. Wassermann, P. Zielke, J.J. Lee, C. Cézard, M.A. Suhm, J. Phys. Chem. A **111**, 7437 (2007)
8. J.J. Hudson, B.E. Sauer, M.R. Tarbut, E.A. Hinds, Phys. Rev. Lett. **89**, 023003 (2002)
9. M. Quack, J. Stohner, M. Willeke, Annu. Rev. Chem. **59**, 741 (2008)
10. J. Cubizolles, T. Bourdel, S.J.J.M.F. Kokkelmans, G.V. Shlyapnikov, C. Salomon, Phys. Rev. Lett. **91**, 240401 (2003)
11. A.N. Nikolov, J.R. Ensher, E.E. Eyler, H. Wang, W.C. Stwalley, P.L. Gould, Phys. Rev. Lett. **84**, 246 (2000)
12. H.L. Bethlem, G. Berden, G. Meijer, Phys. Rev. Lett. **83**, 1558 (1999)
13. S.D. Hogan, Ch. Seiler, F. Merkt, Phys. Rev. Lett. **103**, 123001 (2009)
14. E. Narevicius, A. Libson, C.G. Parthey, I. Chavez, J. Narevicius, U. Even, M.G. Raizen, Phys. Rev. A **77**, 051401 (2008)
15. M.R. Tarbutt, H.L. Bethlem, J.J. Hudson, V.L. Ryabov, V.A. Ryzhov, B.E. Sauer, G. Meijer, E.A. Hinds, Phys. Rev. Lett. **92**, 173002 (2004)
16. R. Fulton, A.I. Bishop, M.N. Shneider, P.F. Barker, J. Phys. B, At. Mol. Opt. Phys. **39**, S1097 (2006)
17. R. Fulton, A.I. Bishop, M.N. Shneider, P.F. Barker, Nat. Phys. **2**, 465 (2006)
18. A.I. Bishop, L. Wang, P.F. Barker, New J. Phys. **12**, 073028 (2010)
19. R. Fulton, A.I. Bishop, P.F. Barker, Phys. Rev. A **71**, 043404 (2005)
20. P.F. Barker, M.N. Shneider, Phys. Rev. A **64**, 033408 (2001)
21. P.F. Barker, M.N. Shneider, Phys. Rev. A **66**, 065402 (2002)
22. M.J. Wright, P.L. Gould, S.D. Gensemer, Rev. Sci. Instrum. **75**, 4718 (2004)
23. Y. Li, S.M. Goldwasser, P.R. Herczfeld, L.M. Narducci, J. Quantum Electron. **42**, 208 (2006)
24. K.S. Repasky, G.W. Switzer, J.L. Carlsten, Rev. Sci. Instrum. **73**, 3154 (2002)
25. J.J. Zayhowski, A. Mooradian, Opt. Lett. **14**, 618 (1989)
26. S. Valling, B. Ståhlberg, A.M. Lindberg, Opt. Laser Technol. **39**, 82 (2007)
27. A.E. Siegman, *Lasers* (University Science Books, Mill Valley, 1986)
28. S. Kobayshi, T. Kimura, J. Quantum Electron. **QE-17**, 681 (1981)
29. M.S. Fee, K. Danzmann, S. Chu, Phys. Rev. A **45**, 4911 (1992)